A PROGRESS REPORT ON THE ULTRASONIC DETECTION OF CAVITIES IN METAL CASTINGS

N. G. Barton

This project is concerned with an important inverse problem - the use of ultrasound to determine the shape of inclusions (or cavities or flaws) in metal castings. This problem is severely ill-posed both analytically and computationally because it is non-linear and because it is an inverse problem in which the shape of the inclusion need not depend continuously on the available far-field data.

The author has been collaborating with the CSIRO Division of Applied Physics on certain theoretical, computational and practical aspects of this inverse problem. This article gives a progress report on the research project from the mathematician's point of view. The discussions on the project held at the 1986 Summer Research Institute of The Australian Mathematical Society are also summarized.

1. Introduction

The task at hand is to determine the shape of small inclusions (bubbles or flaws) in metal castings. This may be classified under the general heading of "non-destructive testing", and the specific motivation for the work was an APIP (Applied Physics Industrial Program) project at the CSIRO Division of Applied Physics. The metal castings under consideration have typical dimensions of 0.1 - 1.0m, whereas the inclusions are very small with typical dimensions of 10^{-4} - 10^{-3}m . The vehicle for the investigation is ultrasound at typical frequencies around 10 MHz with wavelengths of about 0.6×10^{-3}m in the castings.

These scales correspond to the so-called "resonance regime" - that is the quantity ka ($k = 2\pi/\text{wavelength}$, a = typical dimension of inclusion) is in the range 1 - 10, and the inclusions are said to "scatter" the incident beam of ultrasound. Inverse problems associated with this regime have been comprehensively surveyed by Colton (1984). [In contrast, the regime in which ka is large is called the "diffraction" regime, and Sleeman (1982) has described the asymptotic analysis required to investigate inverse problems in this case. The remaining case, in which ka is small, must be approached using perturbation methods; it has not, to the author's knowledge, been the subject of a survey article.]

It is necessary to consider the acquisition of data. The laboratory set-up is displayed in Figure 1. The experiments are performed in a water bath for two reasons: ultrasound is much less attenuated by water than air and the water provides a lower acoustic impedance mismatch to the casting than would experiments with air as the surrounding medium. At present, a movable transducer placed close to the casting emits a short pulse (of duration $2 - 3 \times 10^{-7}$ sec) of ultrasound containing a band of frequencies around 10 MHz, and the scattered ultrasound is detected either by the same transducer or by another movable transducer also placed close to the casting surface.

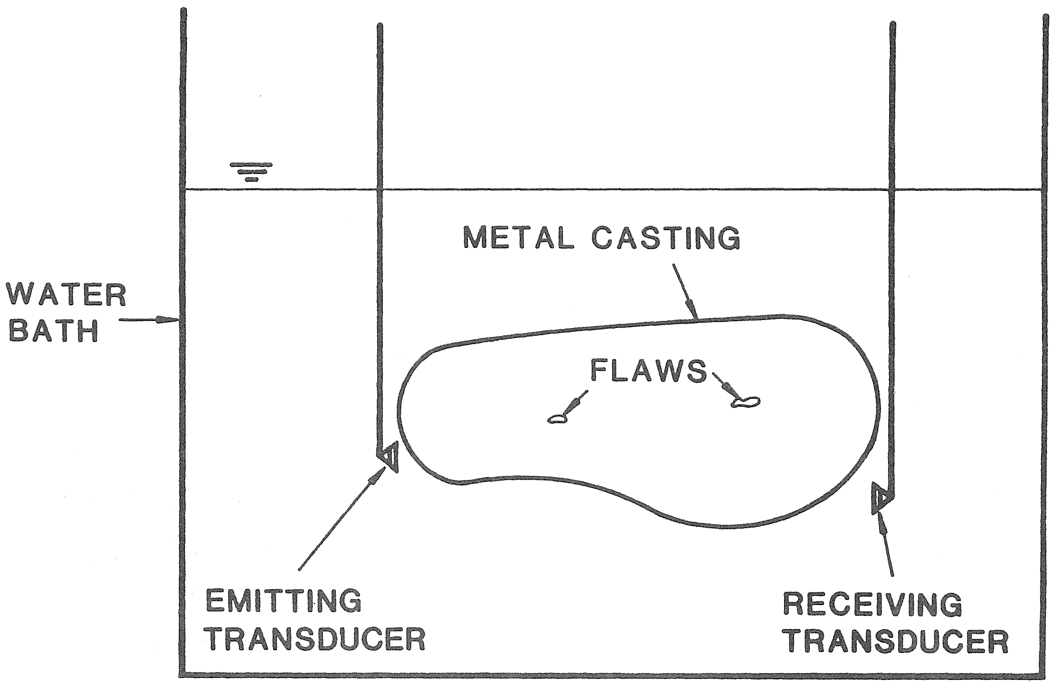

Figure 1. Illustration of the present experimental set-up. Both transducers are movable.

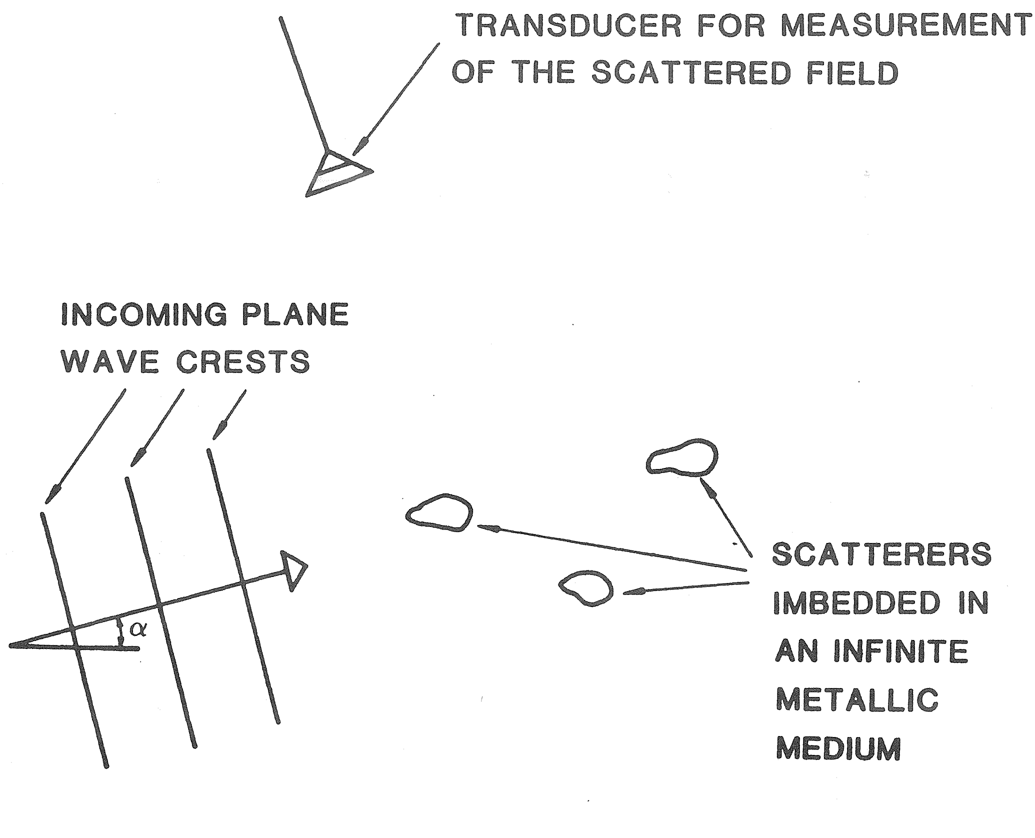

Figure 2. The idealised set-up. Plane waves moving in the direction α impinge on the inclusion(s). The scattered ultrasonic field $|u_s|$ is detected by a movable transducer. The incident ultrasound could be replaced by a conical beam without loss of generality.

Two major assumptions are now made to facilitate the formulation of a tractable inverse problem. First, the generation of a pulse containing one dominant frequency is experimentally possible, and this is from henceforth considered to be the usual operation of the apparatus. Secondly, it is hypothesized that the metal casting extends to infinity. This assumption leads to major simplifications, but neglects the importance of several difficulties such as sound transmission across the interface between the transducer and the casting, the effect of inhomogeneities in the casting, and echoes and reflections of the beam from the surface of the casting. [The caption to Figure 9 shows how the need for this second assumption is avoided in practice.] Therefore the idealized ultrasound problem sketched in Figure 2 is now considered.

The inverse problem at the heart of this work is as follows: given the simplified situation displayed in Figure 2, determine the shape of the inclusion(s) from measurements by the receiving transducer of the total scattered ultrasound field. The equation which governs the scattering is Helmholtz's equation as explained in Section 2. Details that are assumed to be known include the nature of the beam from the emitting transducer, the nature of the impedance mismatch (and hence the relevant boundary conditions) at the boundary of the inclusion, and the acoustical properties of the metal casting.

It is necessary to mention again the important review paper on this topic by Colton (1984) and the more detailed monograph by Colton and Kress (1983). It is not intended to repeat their theoretical analysis, rather the goal of this research is to examine some of the computational and practical aspects of the inverse problem. It is, however, important to mention Colton's conclusions that the inverse problem is difficult to solve because it is non-linear and ill-posed. Indeed, there is very little theoretical support for the computational aspects of the inverse problem. For example, there appears to be no theory available for multiple scatterers, or for single scatterers which are either of complex shape or not simply connected. In addition, numerical work on the inverse problem is, as yet, rudimentary.

Section 2 describes the existing mathematical theory on the inverse problem as presented by Colton, whilst Section 3 describes the literature of computational work on the both direct and inverse acoustic problems. Section 3 also contains a progress report on the author's numerical work on the two dimensional direct and inverse problems. Section 4 describes the experimental technique known as the "synthetic aperture" method at present used by the CSIRO Division of Applied Physics to study the inverse problem. The key recommendations made during the 1986 Summer Research Institute are presented in Section 5 and a short discussion in Section 6 summarises the present state of this interesting research project.

2. The Mathematical Theory

Acoustic wave propagation in a homogeneous, isotropic medium with density ρ and speed of sound c is now considered. The velocity field $\mathbf{v}$ and associated pressure field p of the wave motion are given by

$$\mathbf{v} = \frac{1}{\rho}\nabla U \; , \; p - p_0 = -\frac{\partial U}{\partial t} \tag{2.1}$$

where U is the velocity potential and p_0 is the pressure of the undisturbed medium. In linear theory, U satisfies the wave equation

$$\frac{\partial^2 U}{\partial t^2} = c^2 \nabla^2 U \,, \tag{2.2}$$

and, if the motion is harmonic in time, the velocity potential may be written as

$$U(x,t) = u(x)\, e^{-i\omega t} \tag{2.3}$$

where the function $u(x)$ satisfies Helmholtz' equation

$$\nabla^2 u + k^2 u = 0 \tag{2.4}$$

with $k^2 = \omega^2/c^2$.

Boundary conditions have to be applied at the boundary of the inclusion and as $|x| \to \infty$. Boundary conditions at the inclusion boundary ∂D may be written as

$$\frac{\partial u}{\partial \nu} + \mu u = 0 \quad \text{on} \quad \partial D \tag{2.5}$$

where ν denotes the unit outward normal on ∂D , and $\mu = i\chi\rho\omega$ where χ is the acoustic impedance of the obstacle D .

Two important simplifications of (2.5) are frequently made. If the total pressure vanishes on ∂D , the obstacle is called sound-soft and (2.5) reduces to

(2.6) $$u = 0 \quad \text{on} \quad \partial D .$$

Alternatively, if the normal component of velocity vanishes on ∂D, the obstacle is sound-hard and (2.5) becomes

(2.7) $$\frac{\partial u}{\partial \nu} = 0 \quad \text{on} \quad \partial D .$$

In expressions (2.5 - 2.7) , u represents the total acoustic field and can be written as $u = u_i + u_s$ where u_i is the incident sound field and u_s is the scattered field. Now the remaining boundary condition is the Sommerfeld Radiation Condition which states that the energy associated with the scattered field u_s must be radiated outwards at infinity. This condition gives

(2.8a) $$\lim_{r\to\infty} r^{1/2}\left[\frac{\partial u_s}{\partial r} - iku_s\right] = 0 , \quad r = |x| , \; x \in \mathbb{R}^2 ,$$

(2.8b) $$\lim_{r\to\infty} r\left[\frac{\partial u_s}{\partial r} - iku_s\right] = 0 , \quad r = |x| , \; x \in \mathbb{R}^3 ,$$

for two and three-dimensional problems respectively.

The direct problem posed by equations (2.4, 2.5, 2.8) possesses a unique solution exterior to D provided that the boundary ∂D is sufficiently smooth in the sense defined precisely by Colton and Kress (1983). For our purposes, it is important to consider the far field properties of the scattered solution. In the three-dimensional case, the scattered solution has the asymptotic behaviour (Colton, 1984)

$$u_s(x) = \frac{e^{ikr}}{r} F(\hat{x};k,\alpha) + O\left(\frac{1}{r^2}\right)$$

where $r \equiv |x|$, $\hat{x} \equiv x/r$, α gives the direction of the incident beam, and F is an analytic function of its variables for x on the unit sphere and $k > 0$. One statement of the inverse problem to be solved is now: given the incident beam u_i , the wavenumber k , the constant μ in the boundary condition (2.5) and the far-field $F(\hat{x};k,\alpha)$ measured for $\hat{x}$ on the unit sphere, determine the shape of the boundary ∂D .

If the far-field f is known exactly, then the following (non-constructive) theorem due to Schiffer guarantees the uniqueness of the scattering obstacle D .

THEOREM (Schiffer) *The scattering obstacle* D *is uniquely determined by a knowledge of the far-field pattern* F *for* $\hat{x}$ *on some surface patch of the unit sphere and for* k *on any interval of the positive real axis.*

Schiffer's theorem does not give any insight into how the obstacle D can be constructed from a knowledge of the far-field pattern, nor does it apply in the practically important case when D consists of several separate scattering objects. Moreover, the ill-posed aspects of the inverse scattering problem are not evident in the statement of the theorem.

We now turn to a summary of the existing mathematical work on the inverse scattering problem. Colton's (1984) survey article describes three possible approaches and these are now presented by introducing the operator $\mathcal{T}$ which maps the boundary ∂D and the incident field u_i into the far field pattern $F(\hat{x},k,\alpha)$. Schiffer's theorem guarantees that if a solution of the inverse problem exists, it is unique; and this establishes the existence of $\mathcal{T}^{-1}$ on $R(\mathcal{T})$ (the range of $\mathcal{T}$) . What is now required is to stabilise the inversion: that is to determine a subset $X \subset R(\mathcal{T})$ and an operator $\hat{\mathcal{T}}^{-1}$ defined on $L^2(\Omega)$ (Ω is the unit sphere in $\mathbb{R}^2$ or $\mathbb{R}^3$) such that $\hat{\mathcal{T}}^{-1} = \mathcal{T}^{-1}$ on X and $\hat{\mathcal{T}}^{-1}$ is continuous on $L^2(\Omega)$. Moreover, a constructive method for determining $\hat{\mathcal{T}}^{-1}x$, $x \in X$, must be found.

The Linearized Problem

If an initial approximation D_0 to the shape of D is known, the calculation of the perturbation $\partial\nu$ along the normal required to give the exact shape of D is a linear problem and can be attacked by a range of methods including the Tikhonov selection method and the Backus-Gilbert method. To illustrate the former, suppose that $\mathcal{T}(\partial D) = F$ and $\mathcal{T}(\partial D_0) = F_0$. If $\partial D - \partial D_0$ is denoted by x and $F - F_0$ by y , the linearized problem to be solved is

$$\mathcal{T}x = \mathcal{T}(\partial D - \partial D_0) \cong \mathcal{T}(\partial D) - \mathcal{T}(\partial D_0) = F - F_0 = y$$

where the mapping $\mathcal{T}x = y$ is now regarded as a linear map provided that x is suitably small. The selection method gives a "solution" of $\mathcal{T}x = y$ by restricting the class of admissible solutions a priori to a compact set $X_0 \subset \text{Domain}(\mathcal{T})$ and defining the "solution" to be that $x_0 \in X_0$ for which

$$\|\mathcal{T}x_0 - y\| = \inf_{x \in X_0} \|\mathcal{T}x - y\| .$$

The implementation of the Backus-Gilbert method for solving the linearized problem requires rather more description however; details and further references are given by Colton (1984).

The Analytic Solution of a Model Inverse Problem

In the special case of two-dimensional problems in which the first N Fourier coefficients of the far field pattern F are known exactly, Colton (1984) has described an analytic method for determining an approximation to the scatterer. The method is based on a recursive determination of the unique analytic function f where $z = f^{-1}(w)$ conformally maps the exterior of the unknown obstacle D onto the exterior of the unit disc. A feature of this method is that it is possible to deduce mean square error estimates of the form

$$\frac{1}{2\pi}\int_0^{2\pi} \left| f(e^{i\theta}) - f_N(e^{i\theta}) \right|^2 d\theta \le a^2/N$$

where f_N is a Laurent series approximation truncated at $(N+1)$ terms and a is a constant known as the mapping radius. However these bounds are only for the truncation error; no such bounds are available for the effect of measurement errors.

Optimal Solutions of the Inverse Scattering Problem

We now consider the case where an approximation to ∂D is not known, and it is desired to invert the mapping $\mathcal{T}(\partial D) = F$. An approximation to ∂D is constructed by minimizing the expression $\|\mathcal{T}(\partial D)-F\|$ where $\|\cdot\|$ denotes the norm on $L^2(\Omega)$ and Ω is the unit sphere in $\mathbb{R}^2$ or $\mathbb{R}^3$. The unknown scattering obstacle ∂D is parameterized by $x = f(\hat{x})\hat{x}$ for $\hat{x} \in \Omega$. If ∂D is restricted to belong to the class $\mathcal{U}$ which is any compact subset of

$$\mathcal{F} = \{f \in C^{1,\alpha}(\Omega) \ : \ \|f\|_{1,\alpha} \leq b \ , \ f(\hat{x}) \geq a\} \ ,$$

then Colton (1984) states theorems which prove that the minimization problem

$$\text{minimize} \quad \|\mathcal{T}(\partial D) - f\| \quad \text{subject to} \quad \partial D \in \mathcal{U}$$

has a solution which depends continuously on the data. In the definition above $C^{1,\alpha}(\Omega)$ denotes the space of Hölder continuously differentiable periodic functions defined on the unit sphere, and the assumptions imply that the unknown obstacle is star-like with respect to the origin, contains a ball of radius a, is contained in a ball of radius b, and that ∂D has a uniformly bounded Hölder continuous tangent.

The above remarks indicate it is theoretically possible to stabilize the inverse scattering problem provided that ∂D is restricted to lie in a suitable control set. It now remains to implement the inversion numerically. In general, this task is performed through non-linear minimization: for example, Colton (1984) and Kirsch (1982) suggest that $f \in \mathcal{U}$ be written as the Fourier expansion

$$f(\theta) = a_0 + \sum_{m=1}^{M} (a_m \cos m\theta + b_m \sin m\theta)$$

where the real numbers (a_m , b_m) are found by minimizing the expression

$$\max_{n=1,\ldots,N} |\sigma_{observed}(k;\alpha_n) - \sigma(k;\alpha_n)|$$

where $\sigma(k;\alpha)$ denotes the scattering cross-section

$$\sigma(k;\alpha) = \int_{\Omega} |F(\hat{x};k,\alpha)|^2 dS .$$

It is not necessary to work with the scattering cross-section σ or even the far field pattern F. Instead the real numbers (a_m , b_m) [or other parameters describing approximations to ∂D] can be selected by minimizing

$$\sum_{j=1}^{J} \sum_{n=1}^{N} \Big| |u_{observed}(k;\alpha_n,\beta_j)| - |u(k;\alpha_n,\beta_j)| \Big|^2$$

where u denotes the total acoustic field measured at angle β_j with an incident beam angle α_n .

No matter which representation is chosen, the task to be performed is a large non-linear minimization in which the direct problem has to be solved at each time step. This direct problem is now addressed.

3. Computational Work on the Direct and Inverse Problems

Again, the reader is referred to Colton (1984) for a more complete discussion of the issues discussed in this section. The solution of the direct problem [that is, compute the scattered field given the shape of the scatterer and the incident sound field] has been well-understood for about 25 years, and there are at least three ways of computing the solution. References are given by Colton (1984) and it is notable that fresh computational results are continually being reported - witness the wok of Tobocman (1984), and Schuster & Smith (1985). Numerical work on the inverse problem is much scarcer, perhaps the most notable work is by Kirsch (1982) and very recently by Colton & Monk (1985).

The Direct Problem

A numerical solution of the two-dimensional direct problem posed by equation (2.4) under the sound-soft boundary condition (2.6) and the Sommerfeld Radiation Condition (2.8a) is now described. For this purpose, the two-dimensional Green's function

$$(3.1) \qquad G(x,y) = \frac{i}{4} H_0^{(1)}(kr) \;, \quad r = |x-y|$$

is introduced, where $H_0^{(1)}$ is the Hankel function of the first kind. The scattered sound field $u_s(x)$ is represented as the combined single and double layer distribution

$$(3.2) \qquad u_s(x) = \int_{\partial D} \left\{ \frac{\partial G(x,y)}{\partial \nu(y)} - iG(x,y) \right\} \psi(y) \, dS(y)$$

where $\nu(y)$ is the outward pointing normal on the boundary ∂D. If the point x is now allowed to approach a point x_0 on ∂D, then, following the standard discontinuity properties of single and double layer distributions, the distribution function $\psi(y)$ must satisfy the integral equation

$$(3.3) \quad \psi(x_0) + 2\int_{\partial D}\left\{\frac{\partial G(x_0,y)}{\partial \nu(y)} - iG(x_0,y)\right\}\psi(y)\, dS(y) = -2u_i(x_0)$$

when the sound-soft boundary condition $u_s(x_0) + u_i(x_0) = 0$ has been invoked. This integral equation (3.3) is known to possess a solution for all k (see Colton (1984) for proof), and it remains to introduce a numerical method to calculate the solution.

The boundary ∂D was discretized by taking values $r_n = r(\theta_n)$ where the θ values $0 < \theta_1 < \theta_2 < \ldots < \theta_N = 2\pi$ were evenly spaced. [It is assumed that enough is known of D to place the centre of the polar co-ordinates inside D.] The integrals in (3.3) are periodic so the trapezoidal rule with evenly spaced intervals was used to approximate them. Where necessary, singular integrals were treated by extracting the singularity and integrating analytically. An example of this is

$$\int_{\partial G} G(x_0,y)\psi(y)dS(y) = \int_{\partial G} G(x_0,y)\left\{\psi(y) - \psi(x_0)\right\}dS(y) + \psi(x_0)\int_{\partial G} G(x_0,y)dS(y)$$

where the first term on the right hand side is non-singular and can be approximated by

$$\sum_{j=1}^{N} a_j \; G(x_0,y_j) \; \{\psi(y_j) - \psi(x_0)\} \; dS(\theta_j)$$

(the a_j are the weights in the trapezoidal rule), and where the singularity in the second term on the right hand side can be evaluated analytically. Thus, equation (3.3) can be replaced by the set of simultaneous equations

$$\sum_{n=1}^{N} A_{mn}\psi(y_n) \;=\; -2u_i(x_{0m}) \;, \quad m=1,\ldots,N \;,$$

with complex-valued coefficients A_{mn} . This system may be solved by standard packages; the package used here is LEQT1C of the IMSL library.

Once the distribution function $\psi(y)$ has been obtained, it is a straightforward matter to evaluate the scattered field $u_s(x)$ using the representation (3.2). In particular, none of the integrals involved are singular when $x \in \mathbb{R}^2\backslash\bar{D}$, and straightforward trapezoidal quadrature is accurate and easy to apply.

Several checks are available on the numerical solution. In particular, trapezoidal and Simpson's rule quadratures were both coded and gave answers that were identical for practical purposes. Also, the numerical work was checked against the special case in which the scatterer was a circle of radius a . In this case, the scattered field is given by the separable solution

$$(3.4a)\quad u_s(r,\theta) = A_0 H_0^{(1)}(kr) + \sum_{m=1}^{\infty} H_m^{(1)}(kr)\,\{A_m \cos m\theta + B_m \sin m\theta\}$$

where

$$(3.4b)\qquad A_0 = -J_0(ka)/H_0^{(1)}(ka) \ ,$$

$$(3.4c)\qquad A_m = -2i^m J_m(ka)/H_m^{(1)}(ka) \ ,$$

$$(3.4d)\qquad B_m = 0$$

Here, the incident sound field corresponds to the plane wave e^{ikx} propagating in the direction of the x axis. The results of these computations are shown in Figure 3, and it is held that an accurate numerical solution of the two-dimensional direct scattering problem is now available.

The Inverse Problem

The inverse problem is a much harder problem to solve numerically since it entails solving the above direct problem a large number of times as is now illustrated. Consider the situation depicted in Figure 4 in which it is desired to estimate the unknown radii $r_1, r_2, \ldots, r_N$ using measurements of the total scattered field $|U_{m\ell}|$ at angles $0 < \beta_1 < \beta_2 < \ldots < \beta_M$ on the circle $r = R$ produced by plane sound waves propagating in the directions $0 < \alpha_1 < \alpha_2 < \ldots < \alpha_L$. That is, to minimize

$$(3.5)\qquad E = \sum_{\ell=1}^{L} \sum_{m=1}^{M} \left\{ |U_{m\ell}| - |u_i + u_s| \right\}^2$$

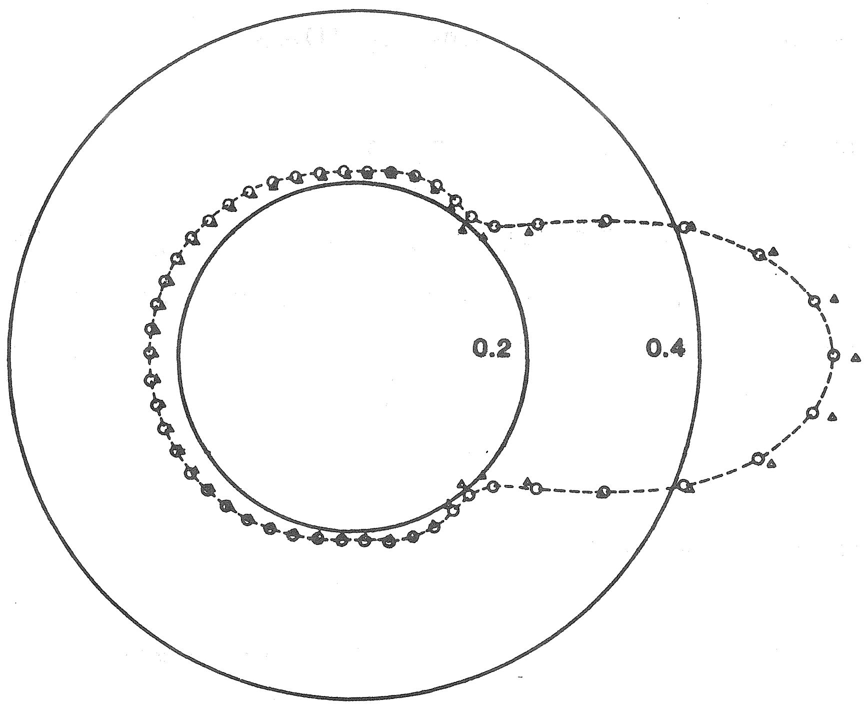

Figure 3. A polar plot of the magnitude $|u_s|$ of the scattered field at radius 10 produced by a plane ultrasound wave impinging on a circular cylinder of radius 1. The incident beam is from the left and the wavenumber k is 3. The dashed line shows the separable solution (3.4), the open circles show the full solution (3.2) whilst the open triangles show the leading far-field approximation to (3.2).

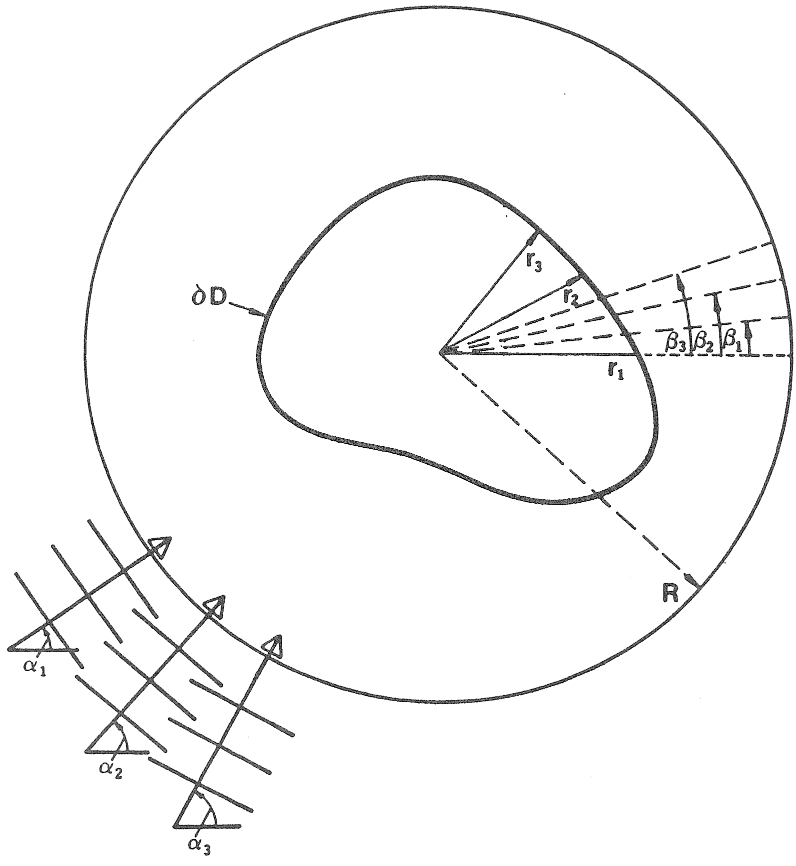

Figure 4. Illustration of a hypothetical inverse problem. The total scattered field is measured at stations $\beta_1, \beta_2, \ldots, \beta_M$ at radius $r = R$. The incident ultrasonic plane waves are propagating in one of the directions $\alpha_1, \alpha_2, \ldots, \alpha_L$; and it is required to determine the unknown coefficients $r_1, r_2, \ldots, r_N$ by minimizing E as defined in equation (3.5).

where $|u_i + u_s|$ denotes the total sound field in which the component u_s is produced by numerically solving the direct problem as explained above. The minimization package LMM was used to minimize E ; it is based on the Levenberg-Marquardt algorithm.

A key step in the minimization routine is the evaluation of the derivatives $\partial\{|u_i + u_s|\}/\partial r_n$ which are required for the convergence of the procedure. The package LMM has an option for these derivatives to be calculated using finite differences, but this option entails the numerical solution of the direct problem for each near set of values $r_1, r_2, \ldots, r_N$. In general, the finite difference option would require of the order of 3N numerical solutions of the direct problem for each stage of the calculations in LMM. This procedure was too time-consuming to be implemented successfully on a VAX 11/750 and comments were invited at the workshop on how to speed up the procedure.

An alternative approach to obtain derivative information was to obtain the derivatives $\partial\{|u_i + u_s|\}/\partial r_n$ analytically. This suggestion is discussed in Section 5.

At the time of the Summer Research Institute, I had realized that the minimization using the finite difference calculations was proceeding too slowly to be practicable, but I had not embarked on the analytical calculation of the derivatives $\partial\{|u_i + u_s|\}/\partial r_n$. Accordingly, therefore, there are no worthwhile results to display for the inverse problem. It is important to note, however, that the inverse problem represents a very large computational task, even without the complications due to the ill-posed nature of the problem. This is because the present formalism requires the direct problem to be solved a large number of times to obtain the solution to the inverse problem.

4. The Synthetic Aperture Method

The inverse problem described in Section 1 is currently being solved in the Division of Applied Physics by a version of the "synthetic aperture" method. This technique is common in electrical engineering (particularly for radar applications) but is probably not so well-known to mathematicians and hence is now briefly described.

Suppose that a transducer is emitting a pulse of ultrasound in a conical beam as shown in Figure 5. The duration of the pulse is τ, the half-power beam width is β, and the speed of the ultrasound is c. Then the resolution ρ_R in the beam direction is given by

$$\rho_R = \frac{1}{2} c\tau$$

as illustrated in Figure 5. If the typical figures of $c = 6000 \text{ m sec}^{-1}$ and $\tau = 2.5 \times 10^{-7}$ sec are substituted, the resolution in the beam direction is $\rho_R = 7.5 \times 10^{-4}$ m.

The resolution in the azimuthal direction is inferior, however, as is also illustrated in Figure 5. The arc-width of the beam is $L \approx \beta R$ where β is the half-power beam width as shown. Now β is given by $\beta \approx \lambda/D$ radians where λ is the wavelength emitted and D is the aperture of the transducer. Hence, the azimuthal resolution is

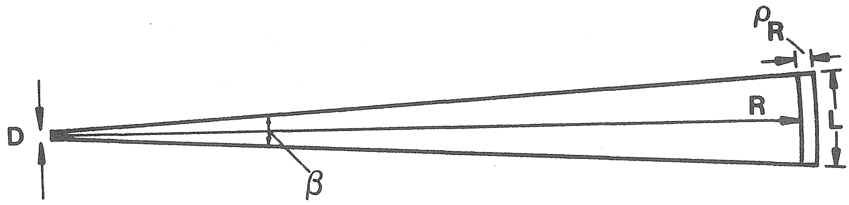

Figure 5. Illustration of the radial and azimuthal resolutions of a pulsed beam. The length of the pulse is τ , so that the radial resolution is $\rho_R = \frac{1}{2} c\tau$ where c is the speed of ultrasound in the medium. The reflected signal could come from the near edge of the zone of resolution and occur at the start of the pulse, or from the far edge at the end of the pulse. The azimuthal resolution is $\rho_A = L$.

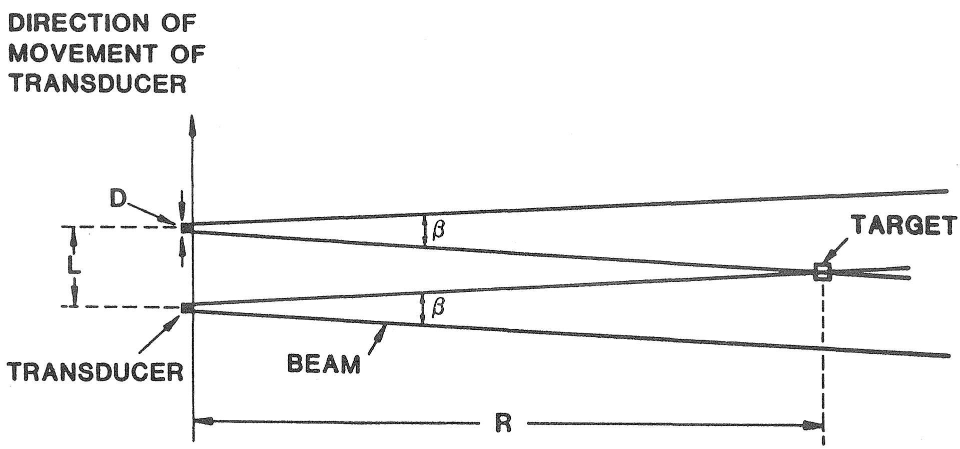

Figure 6. The synthetic aperture method. The actual aperture of the transducer is D and the synthetic aperture is L .

$\rho_A = L \approx \beta R \approx \lambda R/D$, and, for the typical values $\lambda = 0.6 \times 10^{-3}$ m , $R = 2.5 \times 10^{-2}$ m , $D = 10^{-3}$ m , we find that $\rho_A = 1.5 \times 10^{-2}$ m which is markedly inferior to the resolution ρ_R in the beam direction.

This poor resolution in the azimuthal direction is improved by the synthetic aperture method which is depicted in Figure 6. Suppose that the location of the transducer is moved in a straight line perpendicular to the direction of the beam. Then the target at range R will reflect a signal whilst the source moves through the distance $L = \beta R$. If the physical transducer is regarded as one element of a linear array extending along the direction of movement, then intuitively it should be possible to synthesize an aperture of width L by storing and processing the signals received. The angular beam width of this synthetic aperture will be $\beta' = \lambda/L = \lambda/\beta R = D/R$ where λ , β and D are as defined in the discussion leading to the derivation of the azimuthal resolution ρ_A . The "azimuthal" resolution ρ'_A of the synthetic array is $\rho'_A = \beta' R = D$. Clearly, the synthetic aperture method can provided excellent "azimuthal" (or along-track) resolution provided that suitable processing of the signals is possible.

Focussing is also possible in this method. Consider the situation of Figure 7 in which a target element is insonified whilst the emitting transducer is at a range of locations $S_1, S_2, \ldots, S_N$. There will be a recorded signal for each of these transducer locations, as shown in Figure 8. After amplitude-weighting and phase-shifting the stored data, it is then possible to sum coherently the processed data to give the synthetic signal produced by the target element. This procedure is outlined in Figure 8, and can be repeated for all of the target elements

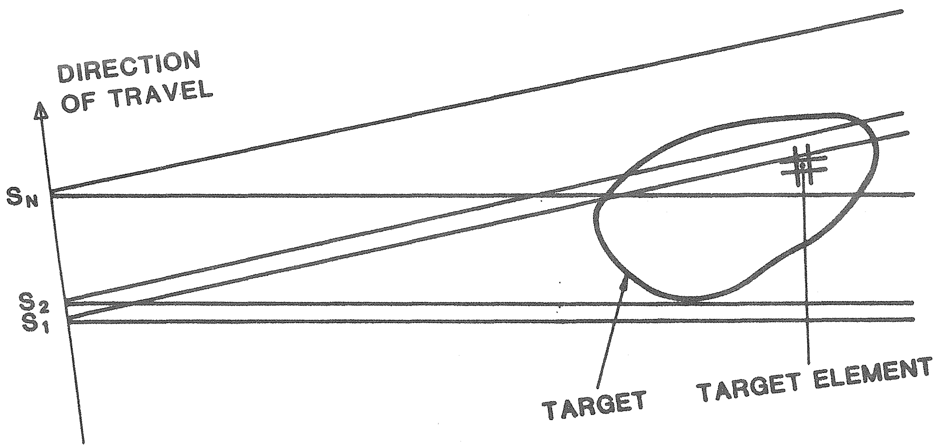

Figure 7. Illustration of transducer locations $S_1, S_2, \ldots, S_N$ and the target element.

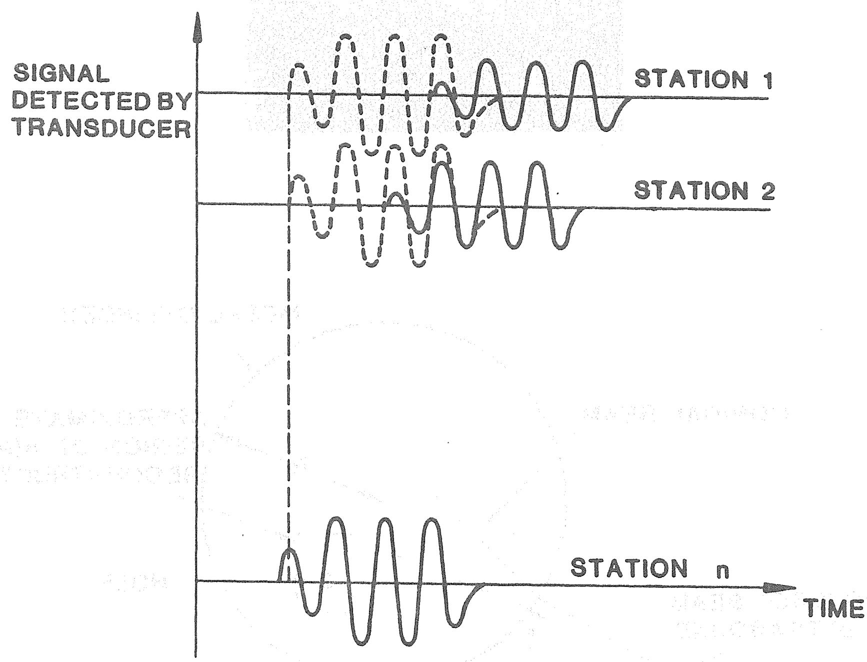

Figure 8. Illustration of the synthesis process. The actual signal received by the transducer is shown by solid lines. These signals are then phase-shifted and amplitude weighted to allow for the fact that the transducer is at a different distance from the target element for each of the transducer locations $S_1, S_2, \ldots, S_N$. This produces the processed signals shown by the dashed lines. [Note that location n $(n<N)$ is used as the reference location - hence the actual and processed signals are identical for this location.] The processed signals are then summed and plotted using an arbitrary scale of intensity.

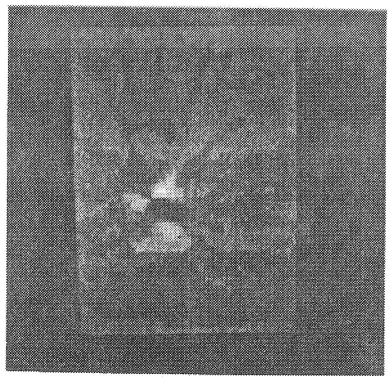

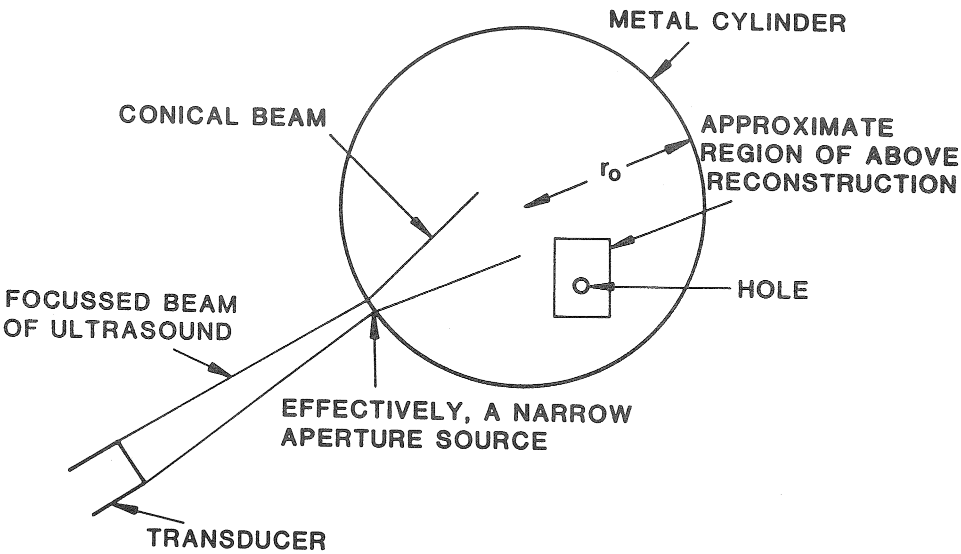

Figure 9. An actual reconstruction. An ultrasound beam is focussed to give a spot of diameter about 1mm on the surface of a cylinder. This spot acts as a narrow aperture source for a conical beam in the cylinder. The signal received back at the spot is picked up by the focussed transducer. The reconstruction of the hole has been squashed in one direction by the plotting algorithm. Other dark zones in the reconstruction are caused by ringing - spurious reflections from the inside of the cylinder.

under consideration. By this process, an image of the object can be built up element by element.

Currently, the Division of Applied Physics is using a variation of this procedure with the emitting transducer moving in a circle rather than in a straight line. Successful image reconstructions have been made; one such is shown in Figure 9, (here the target consists of a cylindrical hole in a metal cylinder).

The synthetic aperture method is in principle no more difficult for 3 dimensions than for 2 dimensions; there is merely more data to be stored and processed, and more target elements to be synthesized. More details on applications of the method in radar have been given by Brown & Porcello (1969) and by Skolnik (1980, ch. 14); it is the basis of operation of side-looking radar mounted on aircraft and satellites.

The synthetic aperture method, as described, relies on a number of simplifying assumptions. The most important of these is that the reconstruction of the image by target elements neglects the fact that the scattering object has an effect on the passage of the emitted and reflected ultrasound. This point does not apply to side-looking radar where the radar signals pass only through air, but it does apply in the ultrasonic application where the object would affect the passage of the ultrasound. Thus there is scope here for an iterative method in which the amplitude-weighting and phase-shifting takes account of what is known of the scatterer's geometry and properties.

5. Discussions during the Summer Research Institute

A number of important comments and suggestions were made during the SRI; and these and the resulting discussions are now summarized here.

5.1 Several suggestions concerned ways in which the procedure described in Section 3 for the numerical solution of the inverse problem could be improved. These included using as much data as could be obtained, using a range of frequencies (further discussion on this point is presented in the next section), and doing the calculations with proper impedance boundary conditions rather than using either the sound-soft or sound-hard boundary conditions. Also, it was pointed out that it should be possible to determine analytically the derivatives $\partial\{|u_i+u_s|\}/\partial r_n$ required in the package LMM . Such an analytical procedure would obviate the need for these derivatives to be approximated using finite differences and would markedly speed up the use of the optimization method for the determination of the $\{r_n\}$. As yet, I have not given consideration as to how these derivatives could be determined analytically. A related suggestion was that information on second derivatives $\partial^2\{|u_i + u_s|\}/\partial r_n \partial r_m$, if available analytically, might be even more useful in speeding up optimization methods for determining the $\{r_n\}$.

5.2 Subsequent discussions with my colleagues in the Division of Applied Physics emphasized the importance of numerical procedures for solving the two or three-dimensional **direct** problem. Experienced users could gain understanding about, although not necessarily solve, inverse problems by using the numerical procedures for direct problems as an investigative tool.

5.3 Some alternative strategies are now outlined. It was suggested that, in many cases, all that would be required would be bulk properties of the scatterer(s), e.g. the location, the volume, and a crude estimate of the shape. It was suggested that such information might be deduced from simple integrals of the data, although I have not yet seen myself how this could be done. However, it should be perfectly possible to replace the scatterer(s) by an equivalent circle or ellipse (in 2 dimensions) or sphere or ellipsoid (in 3 dimensions). All of these geometries lead to separable solutions of Helmholtz' equation in appropriate co-ordinates, and it would be a relatively simple matter to fit the scatterer using these simple geometries. For example, in 2 dimensions, the use of a circle to model the scatterer(s) would require a 3 parameter fit to data (2 parameters to give the location of the centre and 1 for the radius), whilst the use of an ellipse would require a 5 parameter fit. This suggestion should have a lot of practical value.

5.4 A more speculative suggestion was whether variational methods could be employed for the inverse problem. It is known, for example, that the variational method known as the Baiocchi transformation (see e.g. Baiocchi et al., 1973) has been spectacularly successful in finding the unknown interface between saturated and unsaturated soil in certain drainage problems for the flow of water through soil. It is possible that a similar variational approach might be useful for the inverse ultrasonic problem.

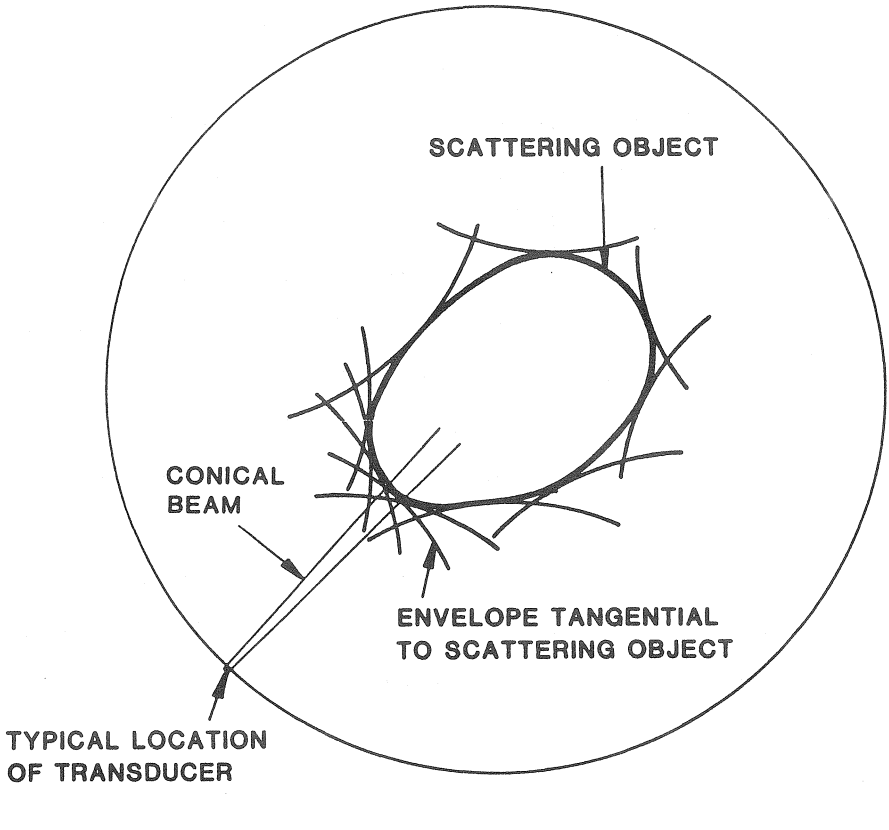

Figure 10. Illustration of an arrival time envelope calculation. The scattering object lies within the envelope of exclusion; as many locations as desired may be taken for the transducer.

5.5 A final ingenious suggestion was to use a simpler version of the (circular) synthetic aperture method. I shall call this new method the arrival time envelope calculation (ATEC). Imagine the situation depicted in Figure 10 in which a transducer which emits a conical beam moves in a circular path with the beam pointing towards the centre. It is known that a scattering object is inside the circle. Then it is a simple matter to use the arrival times of reflected signals to determine a spherical envelope within which the scatterer cannot be situated. This procedure can be repeated for any location of the transducer, and an envelope of exclusion for the scatterer can be built up as shown in Figure 10. This method is simple to implement and should be particularly useful for studies at shorter wavelengths. [Note that if k is the wavenumber of the ultrasound and a is a typical dimension of the scatterer, then ka of $O(1)$ denotes the so-called "resonance region" whereas $ka \gg 1$ denotes the short wave asymptotic region. The ATEC method should be useful for ka moderate up to ka large.] The ATEC method would not be useful for a non-convex scatterer, and would be difficult to apply for multiple scatterers. Still, most other methods also have some difficulty with these cases.

6. Discussion

The content of this article has not been particularly mathematical. This is because the planned mathematical work is incomplete and the rest of the article is concerned with ideas and suggestions for future work. The article describes the state of the project at the time of the Summer Research Institute.

The ultrasonic inverse problem is under active development overseas. A particularly striking example of current work is that of Colton & Monk (1985) who have used a variable wavelength method to solve the inverse problem as a non-linear optimization problem without recourse to the use of integral equations. The method is spectacularly fast in execution.

From our point of view, the suggestions intemized in the previous section are the fruits of the meeting at the SRI. Work is continuing on the inverse problem, and the suggestions are under investigation.

Approximately 3-4 man years of work have been applied to the ultrasonic non-destructive testing project by the CSIRO Division of Applied Physics. Three-dimensional reconstructions have been made using the synthetic aperture method. It is hoped that a prototype instrument for ultrasonic non-destructive testing will be developed over the next two years. This instrument would have an important place in industry and could, hopefully, be commercialized.

I would like to conclude by thanking the participants for their comments at the meeting, and by acknowledging the contributions of my colleagues Dr D C Price (CSIRO Div. Applied Physics) and Ms M Masuda (CSIRO Div. Maths & Stats) to this article.

REFERENCES

[1] Baiocchi, C., Comincioli, V., Guerri, L. & Volpi, G. "*Free boundary problems in the theory of fluid flow through porous media: a numerical approximation*", Calcalo 10 (1973), 1-85.

[2] Brown, William M. & Porcello, Leonard J. "*An introduction to synthetic-aperture radar*", IEEE Spectrum (September 1969), 52-62.

[3] Colton, David. "*The inverse scattering problem for time-harmonic acoustic waves*", SIAM Revue 26 (1984), 323-350.

[4] Colton, D. & Kress, R. "*Integral Equation Methods in Scattering Theory*",(Wiley, N.Y., 1983).

[5] Colton, David & Monk, Peter. "*A novel method for solving the inverse scattering problem for time-harmonic acoustic waves in the resonance region*", SIAM J. Appl. Math. 45 (1985), 1039-1053.

[6] Kirsch, A. "*A numerical method for an inverse scattering problem*", Univ. Delaware, Appl. Math. Inst. Tech. Rpt 127A (1982).

[7] Schuster, Gerard T. & Smith, Lance C. "*A comparison of four direct boundary integral methods*", J. Acoust. Soc. Am. 77 (1985), 850-864.

[8] Skolnik, Merrill I. "*Introduction to Radar Systems*" (McGraw-Hill, 2nd ed., 1980).

[9] Sleeman, B. D. "*The inverse problem of acoustic scattering*", IMA J. Appl. Math. 29 (1982), 113-142.

[10] Tobocman, W. "*Calculation of acoustic wave scattering by means of the Helmholtz integral equation*". Part 1, J. Acoust. Soc. Am. 76 (1984), 599-607; Part 2, J. Acoust. Soc. Am. 76 (1984), 1549-1554.

Division of Mathematics and Statistics
CSIRO
PO Box 218
Lindfield NSW 2070